

Effect of Shear-Span Corrosion on the Flexural Behavior of Repaired RC Beams

Hesham F. Elhuni¹, Khaled A. Soudki²

¹MASc Student, Department of Civil Engineering, University of Waterloo, Waterloo, ON, Canada

²Professor and Canada Research Chair, Department of Civil Engineering, University of Waterloo, Waterloo, ON, Canada

ABSTRACT: This paper examined the effects of corrosion of the longitudinal reinforcement in the shear span on the structural behavior of RC beams and the effectiveness of two rehabilitation schemes. The test variables included: span to depth ratio ($a/d=2.4$ and 3.4), anchorage end condition (anchored and unanchored), the degree of corrosion (2.5%, 5%, 7.5%), and repair schemes (patch repair GFRCM U wraps). Test results showed no major effect of shear-span corrosion on the flexural behavior for the beams with end anchorage whereas a noticeable effect on the flexural behavior was observed for beams with no end anchorage. The type of repair significantly affected the overall behavior of the repaired-corroded specimens.

1 INTRODUCTION

The functionality of a reinforced concrete member under loads depends on the composite action (bond) between the reinforcing steel and concrete (FIB 2000). Corrosion of steel rebars in reinforced concrete is the main cause of concrete deterioration (Nossoni 2010, Wang 2010, and Soudki 2010). Bond loss between concrete and the reinforcement as well as the reduction in the steel rebar cross sectional area of steel are key factors that lead to loss of serviceability (Sahamitmongkol 2007, Nossoni 2010, and Wang 2010). The effect of corrosion of the tensile reinforcement on the structural behavior of RC beams has been researched extensively over the past twenty years. In most of the previous research, the full length of the longitudinal rebar was corroded (Soudki and Sherwood 2000; Masoud and Soudki 2000; El Maaddawy and Soudki 2005; Craig and Soudki 2005). However, in real life localized portions of the rebar may be corroded, and the corrosion damage within a certain length of the RC element may have more pronounced effect on the residual strength of RC structural element. Badawi and Soudki (2010) investigated the effect of shear span corrosion of the longitudinal reinforcement on the structural performance of RC beams with hooked end anchorages. They reported that shear-span corrosion, with properly anchored tension reinforcement, has an insignificant effect on the flexural behavior of RC beams. Wang et al (2011) investigated the effect of localized corrosion damage in one shear span on the shear behavior of RC beams. Their results indicated that high localized corrosion damage within the shear span greatly affected the structural behavior of the test specimens. The studies in the literature conducted on the effect of corrosion in the shear span on structural behavior of RC beams reported contradictory results. Therefore, this study aims to address this controversy in the published literature on the effects of localized corrosion on the structural behavior of RC beams.

2 EXPERIMENTAL WORK

2.1 Test Program

Nine medium-scale reinforced concrete beams were tested to investigate the effect of shear span corrosion on the structural performance of RC beams. Eight specimens were corroded and one specimen was kept un-corroded as a reference. Table 1 summarizes the test matrix. Two span to depth ratios were selected: 3.4 with three point bending and 2.4 with four point bending. Two anchorage end-conditions were chosen: Anchored specimens that were designed to fail in flexure in which the reinforcement in the anchorage zone was bonded and none anchored specimens that were designed to fail in bond, in which the reinforcement in the end anchorage zone was intentionally un-bonded by means of using an aluminum tube over the reinforcing bar. Three degrees of corrosion were chosen to simulate minor (2.5% and 5%) and medium (7.5%) mass losses in the steel rebar. Two repair scenarios were used: 1) applying a composite glass fiber reinforcing cement based matrix (GFRCM) u-wrap and 2) a patch repair.

2.2 Specimen configuration

Figure 1 shows the specimen configuration and reinforcement details. All beams had the same geometry: rectangular cross-section (350mm depth x 150mm width) with a length of 2400 mm. Each beam was reinforced with two 25M deformed bars (bottom reinforcement) with a 40mm clear cover from the bottom and 25mm from the sides. Two 10M deformed bars were used as top reinforcement with 30mm cover from the top and 25mm from the sides. The shear reinforcement consisted of 10M epoxy coated stirrups (for corrosion protection) spaced at 200mm c/c. A hollow 8mm diameter stainless steel bar was placed at a distance of 90mm from the bottom of the specimen to act as the cathode in the accelerated corrosion circuit. Both the bottom reinforcement bars and the stainless steel tube were extended 100mm from one end of the beam to provide sufficient length for connecting the electrical circuit. NaCl was added to the concrete during casting in one shear span of each specimen. The salted shear zone had a length of 1000mm and a height of 110 mm from the bottom face of the specimen.

Table 1: Test matrix

Beam	Depth to span ratio (a/d)	Mass loss (%)	Anchorage condition	Repair scenario
A-C0%-U-3B	3.4	0	anchored	none
A-C2.5-U-3B	3.4	2.5	anchored	none
A-C5-U-3B	3.4	5	anchored	none
A-C7.5-U-3B	3.4	7.5	anchored	none
N-C7.5-U-3B	3.4	7.5	Non-anchored	none
A-C7.5-U-4B	2.4	7.5	anchored	none
N-C7.5-U-4B	2.4	7.5	Non-anchored	none
N-C7.5-R(GFRCM)-4B	2.4	7.5	Non-anchored	U-wrapping
N-C7.5-R(P)-4B	2.4	7.5	Non-anchored	Patch

The specimen designation is as follows: First letter: A or N refers to the anchored (bonded end zone) specimens and the non-anchored (un-bonded end zone) specimens. Second letter/number: C# refers to the corrosion level of: 0, 2.5, 5, and 7.5% mass loss. Third letter: U refers to the unrepaired specimen, R refers to the repaired specimens. GFRCM refers to the specimen wrapped with glass fiber reinforced cement based matrix. P refers to specimen repaired by concrete patch. The last letter: B refers to the loading configuration; 3B represents 3 point bending case with a/d of 3.4 and 4B represents 4 point bending case with a/d of 2.4.

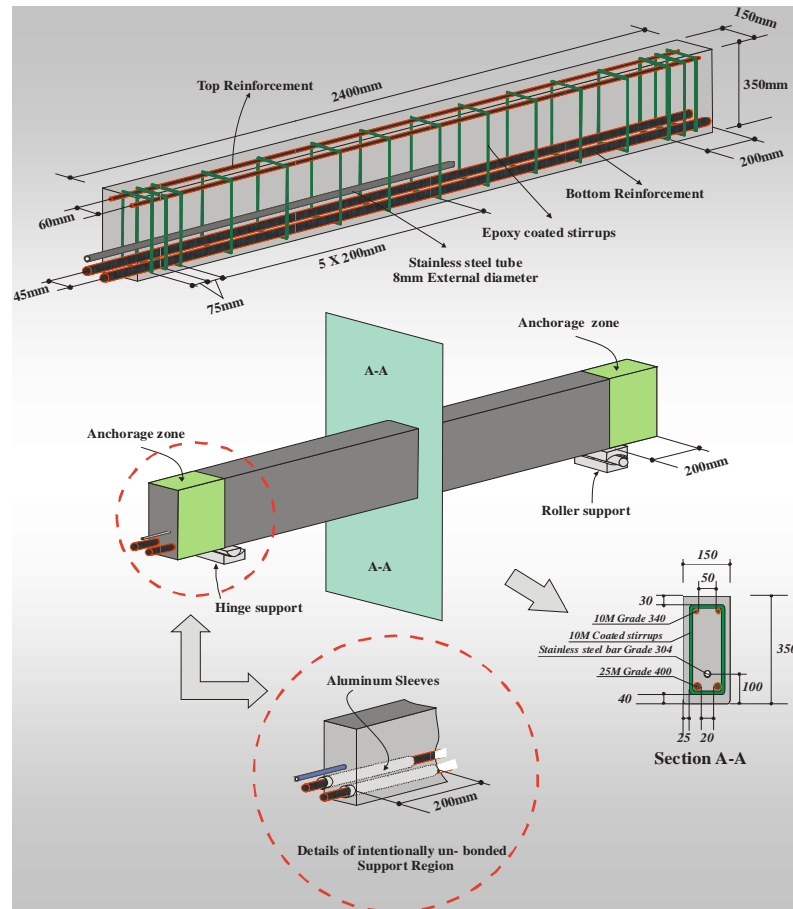


Figure 1. Specimen configuration and reinforcement (all dimensions in millimeters)

2.3 Concrete Mix and Steel Reinforcement

Two concrete mixes, unsalted and salted, were used with a water cement ratio (w/c) of 0.55, and maximum aggregate size of 13mm. The salted mix had a 2.15% of chloride (Cl⁻) by weight of cement. The 28-day average compressive strength the concrete was 49MPa. The reinforcing steel rebar has a yield strength of 400MPa. The yield strength for the stirrups was 320MPa.

2.4 Repair Materials

2.4.1 Composite repair

A composite system was used as an external U-wrap around the beam's cross section in the corroded shear span. The system was composed of a glass fiber mesh and matrix manufactured by Sika Canada, Inc. The glass fiber mesh (Sika Wrap-350G) had a grid size of 30mm by 30mm, a width of 2mm, and thickness of 0.25mm. The matrix was polymer modified cement.

2.4.2 Patch repair

The patch repair material was a Self-Consolidated concrete (Sikacrete-08) manufactured by Sika Canada, Inc. The patch repair was applied to one specimen following the manufacture's

specifications and the recommendations provided by the Concrete Repair Guide (ACI 546R-04). The deteriorated concrete was removed then the concrete area was sandblasted and the surface was saturated before applying the patch repair. Then the specimens were cured for 15 days. The 28 days average compressive strength for the patch concrete was 51MPa.

2.5 Test Procedure

The specimens were subjected to accelerated corrosion according to Faraday's law with a constant current density of $200 \mu\text{A}/\text{cm}^2$ to achieve different corrosion levels: 2.5%, 5%, and 7.5% corrosion mass loss. Following the corrosion exposure, the specimens were tested monotonically to failure at a rate of loading of 3mm/min. Five beams were loaded in three point-bending with a shear span to depth ratio of 3.4 and four beams were loaded in four point bending with a shear span to depth ratio of 2.4. Three LVDTs were used to record the displacements. One vertical LVDT, with a range of 50mm and an accuracy of 0.01mm, was used to measure the vertical mid span deflection. Two horizontal LVDTs, with a range of 25mm and an accuracy of 0.01mm, were used to measure the free end slip in the two reinforcing bars.

3 EXPERIMENTAL RESULTS AND DISCUSSION

Table 2 presents a summary of the test results. Figure 2 shows the typical cracking patterns at failure. Figures 3 to 5 shows the effects of corrosion in anchored longitudinal reinforcement, effect of intentionally non-anchored longitudinal reinforcement and effect of repair systems.

Table 2: Detailed test results for the specimens

Beam	Actual mass loss (%)	Mode of failure	Crack patterns	Ultimate Load (KN)	Yielding Load (KN)	Ultimate deflection (mm)	Ultimate end-slip (mm)
A-C0-U-3B	0	flexure	1	250	209	23	≈ 0
A-C2.5-U-3B	1.52	flexure	2	239	224	17	≈ 0
A-C5-U-3B	3.54	flexure	2	255	214	17	≈ 0
A-C7.5-U-3B	7.36	flexure	2	244	212	22	≈ 0
N-C7.5-U-3B	7.31	flexure	3	260	222	17	≈ 0
A-C7.5-U-4B	8.27	flexure	2	322	300	13	≈ 0
N-C7.5-U-4B	6.71	flexure	3	323	305	17	0.33
N-C7.5-R(GFRCM)-4B	7.13	flexure	4	317	290	>50	0.2
N-C7.5-R(P)-4B	7.34	bond	5	276	-	8	1.5

Refer to Figure 3 for a schematic of crack patterns.

3.1 Corrosion Results

After corrosion and load testing, eight 200 mm long coupons, four from each bar, were extracted from the corroded bars in each specimen. The steel coupons were cleaned according to ASTM standard G1-90 [16]. The mass loss for the steel bars was calculated as the average of the mass losses of coupons extracted from the two bottom steel rebars. Table 2 presents the average mass losses for all the specimens. It is evident that Faraday's law overestimated the steel mass loss for all corrosion levels. This is attributed to the barrier that formed by the corrosion products around the reinforcing rebars which prevent water and oxygen from reaching the steel surface and thus slowed the corrosion process.

3.2 Loading Crack Patterns

The unrepaired beams failed in flexure by concrete crushing after steel yielding. The GFRCM repaired beam (N-C7.5-R(GFRCM)-4B) also exhibited flexural failure in the un-corroded unrepaired span and no fiber rupture was observed. The patch repaired beam (N-C7.5-R(P)-4B) failed by bond splitting in the non-anchored zone, close to the support. The crack patterns varied depending on the anchorage condition, the repair scheme, and the load configuration. For the control (un-corroded, one point load) beam, flexural cracks started to appear in the mid span followed by flexural-shear and shear cracks along the span. The corroded unrepaired beams had less number of cracks in the corroded shear span. This was primarily due to the fact that loading cracks intercepted with the longitudinal corrosion crack. The beams repaired by patching had radial cracks around the main rebars in the anchorage zone and a diagonal shear crack in the support region of the corroded shear span. Figure 2 illustrates the typical crack patterns due to loading for the test specimens.

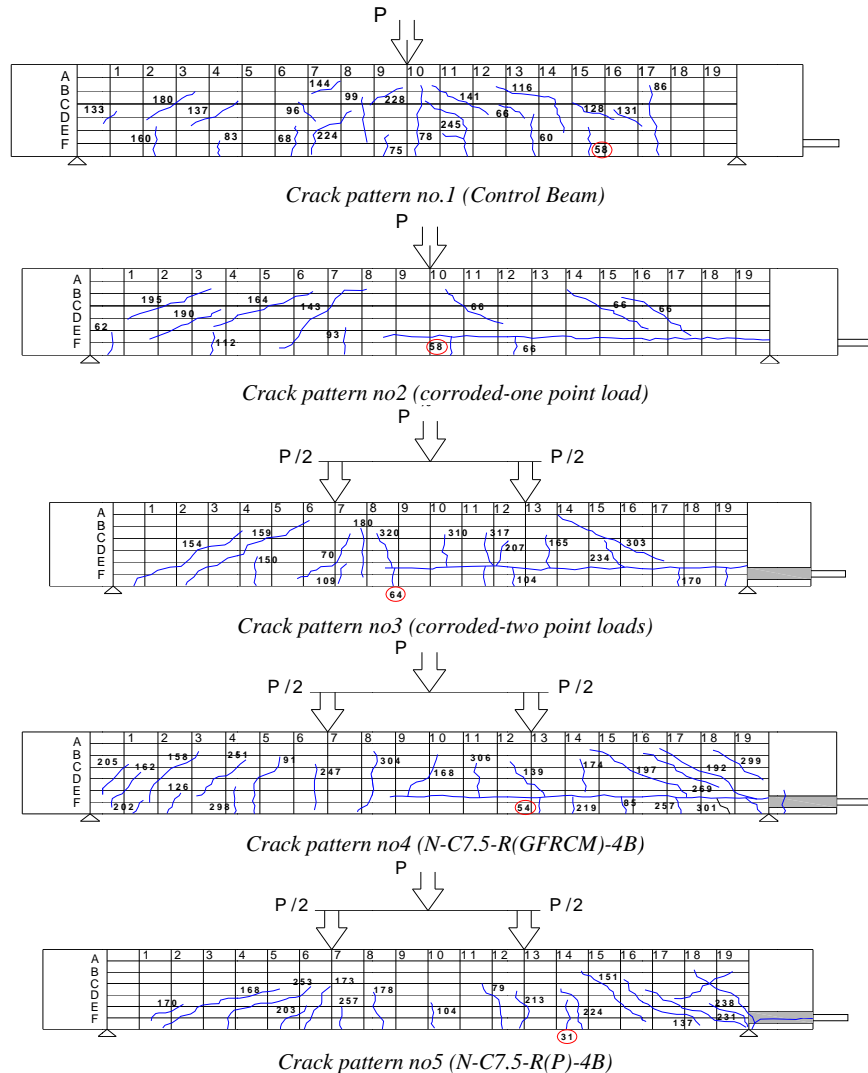


Figure 2 Loading crack patterns

3.3 Effect of corrosion in anchored longitudinal reinforcement

Figure 3 shows the load-deflection curves for the shear span corroded beams with properly anchored longitudinal reinforcement. The yield load of the corroded beams was not affected by corrosion with the reduction in the range of 1.4-7.2%. The ultimate loads were also not affected by shear span corrosion with the reduction in ultimate load in the range of 2-4.4%. This can be explained by the fact that the reinforcement was fully bonded in the anchorage zone and because the beams failed in flexure at mid span (un-corroded zone). The shear-span corrosion slightly increased the flexural stiffness of the beams in the range of 5.7-7.1%.

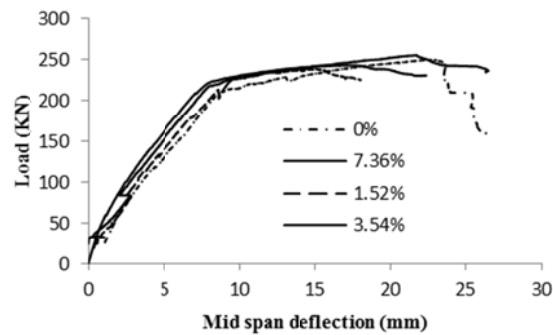
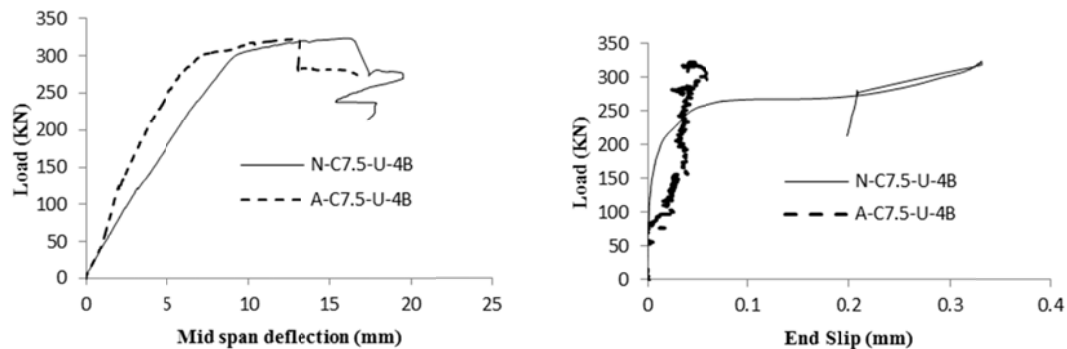


Fig. 3 Effect of corrosion in anchored beams

3.4 Effect of intentionally non-anchored longitudinal reinforcement

Figure 4a shows the load deflection curves for two beams with properly anchored reinforcement (A-C7.5-U-4B) and intentionally non anchored reinforcement (N-C7.5-U-4B). Since the shear span corrosion did not affect the structural behavior of the specimens, beam A-C7.5-U-4B is considered as a control beam for the beam N-C7.5-U-4B. The yield and ultimate loads were not affected by using intentionally non-anchored longitudinal reinforcement. However, it is evident that the beam with no end anchorage experienced pronounced decrease in the flexural stiffness. The reduction in the flexural stiffness was 28.6%. The deflection at failure of the beam with non-anchored reinforcement was 30% higher than that of the beam with anchored reinforcement. This can be explained by examining Figure 4b. The beam with non-anchored reinforcement started to slip close to failure due to loss of bond at the anchorage zone.



(a) Load-deflection

(b) Slip behavior

Fig. 4 Effect of anchorage condition: anchorage vs. non anchored

3.5 Effect of repair systems

Figures 5a and 5b show the load-deflection curves and the load-end slip curves for three beams: corroded un-repaired (as a control), corroded patch repaired, and corroded GFRCM repaired. These three beams exhibited similar steel mass losses (Table 2). The patch repair had an adverse effect on the mode of failure and, therefore, on the flexural response. This could be attributed to partially losing the bond between the cleaned/corroded rebar and the patch concrete. The small aggregate size of the new patch (0-8mm) compared to the sound concrete (13mm) reduced the friction component of the bond strength. The sandblasting reduced the height of the reinforcement ribs which reduced the mechanical interlock component of the bond strength. The patch repaired beam experienced a relatively large end slip, because of the bond loss at the concrete-steel interface. The reduction in the load capacity was 14.6% and the reduction in deflection at failure was 53%. The failure mode changed from a ductile flexural failure to a brittle failure. The stiffness of the beams was not affected by the patch repair. This was because the patch concrete has the same compressive strength as the sound concrete. The GFRCM system was able to significantly enhance the ductility of the repaired beam and provide post-ultimate flexural capacity after the crushing of the concrete. However, the GFRCM system did not affect the yielding load, and the ultimate load. As the composite repair was able to increase the beam ductility, the beam exhibited a small end slip.

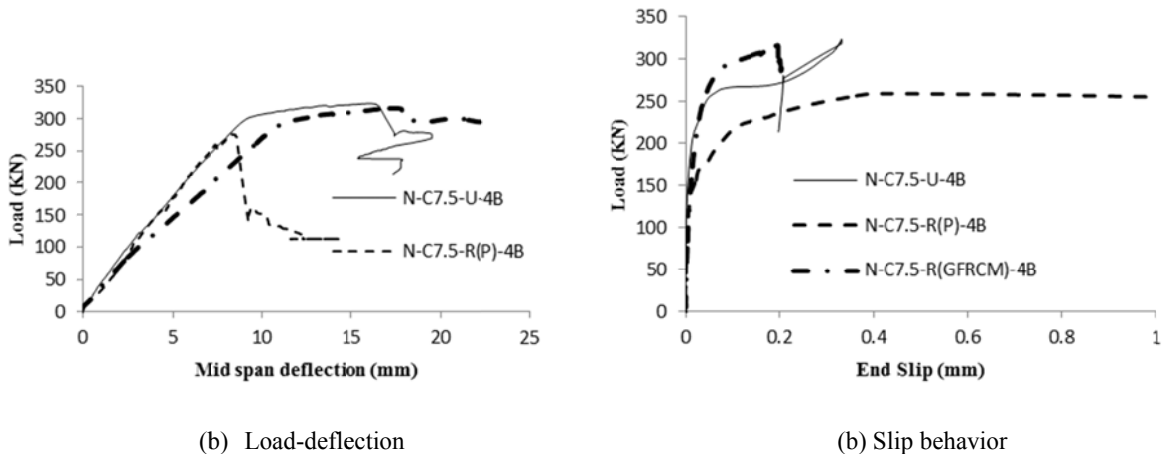


Fig. 5 Effect of repair scenario: Patched vs. GFRCM

4 CONCLUSIONS

This study examined the effects of the shear span corrosion, inadequate end anchorage of the tension reinforcement, and different repair scenarios on the structural behavior of the RC beams. The following conclusions can be drawn from this study:

- Corrosion of longitudinal reinforcement in the shear span did not have a significant effect on the structural behavior of RC beams with properly anchored longitudinal reinforcement. The maximum changes in yielding and ultimate loads were 7.2% and 4% respectively. The maximum change in flexural stiffness was 7.1%
- Corrosion of intentionally un-bonded reinforcement in the anchorage zone significantly reduced the stiffness of shear span corroded RC beams. The reduction in stiffness was 28.6%. The end slip was noticeably increased.

- The GFRCM repair enhanced the flexural ductility of RC beam with shear span corrosion and improperly anchored longitudinal reinforcement. The increase in section ductility was up to 40%. The yield and ultimate loads were not affected by this strengthening system.
- The patch repair had an adverse effect on the flexural behavior and the mode of failure of RC beam with shear span corrosion and improperly anchored longitudinal reinforcement. The ultimate load decreased by 14.6% and the deflection at ultimate was reduced by 53%. The mode of failure was dramatically changed from a ductile flexural failure to bond splitting failure.

5 REFERENCES

- Badawi, M., & Soudki, K. 2010. CFRP repair of RC beams with shear-span and full-span corrosions. *Journal of Composites for Construction*, 14: 323-335.
- El Maaddawy, T. a. 2005. Modelling the non-linear flexural response of corroded and FRP- repaired beams. *Fourth Middle East Symposium on Structural Composites for Infrastructure Applications*, 20-23. Alexandria, Egypt.
- Fib, 2000, Bond of Reinforcement in Concrete, State-of-the-art Report, Bulletin 10, *fib-International Federation for Structural Concrete*, Lausanne.
- Masoud, S., & Soudki, K.A. 2000. Serviceability of corroded carbon fibre reinforced polymer strengthened reinforced concrete beams. *Proceedings of 3rd Structural Speciality Conference of the Canadian Society for Civil Engineering*, 507-514. London.
- Malumbela, G., Moyo, P., & Alexander, M. 2011. Load-bearing capacity of corroded, patched and FRP-repaired RC beams. *Magazine of Concrete Research*, 63: 797-812.
- Nossoni, G., & Harichandran, R. S. 2010. Improved repair of concrete structures using polymer concrete patch and frp overlay. *Journal of Materials in Civil Engineering*, 22: 314-322.
- Soudki, K., El-Salakawy, E., & Craig, B. 2007. Behavior of CFRP strengthened reinforced concrete beams in corrosive environment. *Journal of Composites for Construction*, 11: 291-298.
- Sahamitmongkol, R., Suwathanangkul, S., Phoothong, P., and Kato, Y., 2008, Flexural behavior of corroded RC members with patch repair-experimental & simulation. *Journal of Advanced Concrete Technology*, 6: 317-336.
- Val, D.V. 2007. Deterioration of Strength of RC Beam due to Corrosion and its Influence on Beam Reliability. *Journal of Structural Engineering*, ASCE, 133: 1297-1306.
- Wang, X., & Liu, X., 2010. Simplified methodology for the evaluation of the residual strength of corroded reinforced concrete beams. *Journal of Performance of Constructed Facilities*, 24: 108-119.
- Wang, X., Gao, X., Li, B., & Deng, B. 2011. Effect of bond and corrosion within partial length on shear behaviour and load capacity of RC beam. *Construction and Building Materials*, 25: 1812-1823.
- Xia, J., Jin, W., & Li, L., 2011. Shear performance of reinforced concrete beams with corroded stirrups in chloride environment. *Corrosion Science*, 53: 1794-1805.